

IMPEDANCES AND WAKES IN ROUND THREE-LAYER CERAMIC WAVEGUIDE*

M. Ivanyan[#], A. Tsakanian, CANDLE, Yerevan, Armenia

Abstract

The round ceramic waveguide with inner and outer thin metal coating is considered. Using the exact methods the longitudinal impedances and potentials are calculated. Identification of the main patterns of changes in their properties by varying the electrodynamic and geometric parameters of the waveguide is performed as well. The possibility of optimizing the parameters of the waveguide for the effective implementation of two-beam acceleration is discussed.

INTRODUCTION

Theoretical possibility of two-beam acceleration in the ceramic waveguide with the smooth inner wall is conditioned by the wall material dielectric properties, which allows to excite waves with the phase velocity close to the speed of light and leads to the exception of application of the braking structures with the complex corrugated longitudinal profile. The idea of using the smooth-wall ceramic waveguide for two-beam acceleration was suggested in Argonne laboratory (USA) [1,2]. The experimental studies in that direction are being performed there [2] and in SLAC (USA) [3].

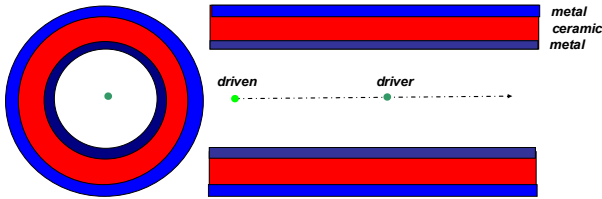


Figure 1. Geometry of the problem

The presence of inner and external metallic layers (Fig.1) is conditioned by the following causes: outer layer prevents the radiation penetration to the external space and turns it back to the axis of structure, amplifies the on-axis field, which accelerates or decelerates the driving bunch. Inner metallic layer prevents the static charge accumulation on the dielectric surface.

For the realization of the two-beam acceleration with the help of the suggested structure it is necessary to solve a lot of problems. The main problem is to obtain the correct electrodynamic solution of moving charge radiation in the structure. Then the geometrical and electrodynamic parameters of the structure should be optimized, related to the maximal acceleration rate achievement. Simultaneously the optimal thermal regime

should be established to avoid the corruption of the structure [3]. Thus, the optimization should be performed with co-ordination of two main tasks mentioned above. The optimization should be performed by geometrical sizes of three-layer waveguide, by the thickness of layers and by choosing the materials of ceramic and metallic layers. This problem needs exact solution of the problem of the moving charged particle radiation in the three-layer tube. The discussed structure (Fig.1) is characterized by radii of the borders between adjoining layers $a_1 < a_2 < a_3 < a_4$ (the layer's numbering starts from the inner layer) and by the electric permittivity ϵ_i and magnetic permeability μ_i of each layer ($i=1,2,3$). In this paper the changes of impedances and wake potentials of the structure with changing its outer metallic layer conductivity and inner metallic layer thickness are investigated. As an example discussed below, the ceramic round tube with unchanged inner and outer radii $a_2=2mm$ and $a_3=4mm$ and relative permeability $\epsilon'_2=2$ is taken. The outer metallic layer thickness is taken equal to $5mm$.

IMPEDANCES

The problem of exact valuation of longitudinal and transverse impedances of multilayer round tube with arbitrary number of layers and finite common thickness was solved in [4]. Matrix method is developed: the properties of each layer are described by the help of 4×4 dimension matrix and the electrodynamic properties of the tube as a whole are presented by the help of the product of the above mentioned matrixes [4].

In particular, for three-layer tube in the ultrarelativistic case the compact expression for the three-layer tube longitudinal impedance, valid for the arbitrary frequencies obtained by the help of matrix method [4] may be presented in the following form:

$$Z_{||} = j \frac{Z_0}{\pi k a_1^2} \left(1 - \frac{2}{k_c a_1} Q \right)^{-1} \quad (1)$$

where

$$Q = \frac{\epsilon_1 k \epsilon_1 \chi_2 U_4^{(1)} V_2^{(3)} - \epsilon_2 \chi_1 U_3^{(1)} V_1^{(3)}}{\epsilon_0 \chi_1 \epsilon_1 \chi_2 U_2^{(1)} V_2^{(3)} - \epsilon_2 \chi_1 U_1^{(1)} V_1^{(3)}} \quad (2)$$

and

$$\begin{aligned} U_1^{(i)} &= K_0(\chi_i a_{i+1}) I_0(\chi_i a_i) - I_0(\chi_i a_{i+1}) K_0(\chi_i a_i) \\ U_2^{(i)} &= K_0(\chi_i a_{i+1}) I_0'(\chi_i a_i) - I_0'(\chi_i a_{i+1}) K_0(\chi_i a_i) \\ U_3^{(i)} &= K_0'(\chi_i a_{i+1}) I_0(\chi_i a_i) - I_0(\chi_i a_{i+1}) K_0'(\chi_i a_i) \\ U_4^{(i)} &= K_0'(\chi_i a_{i+1}) I_0'(\chi_i a_i) - I_0'(\chi_i a_{i+1}) K_0'(\chi_i a_i) \end{aligned} \quad (3)$$

*Work is performed under Contract 10-3/28 of State Committee of Science of Armenia.

[#]ivanian@asls.candle.am

$$\begin{aligned} V_1^{(i)} &= U_1^{(2)}U_4^{(3)}\chi_2\varepsilon_3 - U_3^{(2)}U_3^{(3)}\chi_3\varepsilon_2 \\ V_2^{(i)} &= U_1^{(2)}U_2^{(3)}\chi_2\varepsilon_3 - U_1^{(2)}U_3^{(3)}\chi_3\varepsilon_2 \end{aligned} \quad (4)$$

Here I_0, K_0 are the modified Bessel functions of the first and second kinds and zero order, $\chi_i = \sqrt{k^2 - \varepsilon_i\mu_i\omega^2}$ are the longitudinal propagation constants for each layer, $k = \omega/c$ is wavenumber, ω frequency and c the speed of light; $\varepsilon_{1,3} = \varepsilon_0 + j\omega/\sigma_{1,3}$ with $\sigma_{1,3}$ the conductivities of outer and inner metallic layers respectively. For the middle dielectric layer $\varepsilon_2 = \varepsilon' \varepsilon_0$. For the loss-less case the relative dielectric constant ε' is a real number.

The further simplification of the above expressions (1)-(4) leads to expressions valid for the case of $kd_2\varepsilon'' \ll 1$ ($d_i = a_{i+1} - a_i, i = 1, 2, 3$ is the corresponding layer thickness) with $\varepsilon'' = \sqrt{\varepsilon' - 1}$ and

$$Q = -\frac{\varepsilon_1 k \operatorname{th}(\chi_1 d_1) + \Psi}{\varepsilon_0 \chi_1 (1 + \Psi \operatorname{th}(\chi_1 d_1))} \quad (5)$$

where

$$\Psi = \frac{\varepsilon_2 \chi_1 j \varepsilon_2 \chi_3 \operatorname{th}(\chi_3 d_3) \operatorname{tg}(k d_2 \varepsilon'') + \varepsilon_3 \chi_2}{\varepsilon_1 \chi_2 \varepsilon_2 \chi_3 \operatorname{th}(\chi_3 d_3) + j \varepsilon_3 \chi_2 \operatorname{tg}(k d_2 \varepsilon'')} \quad (6)$$

Figure 2 presented below, shows the longitudinal impedance of the ceramic tube without any inner layer and with different external layers conductivity.

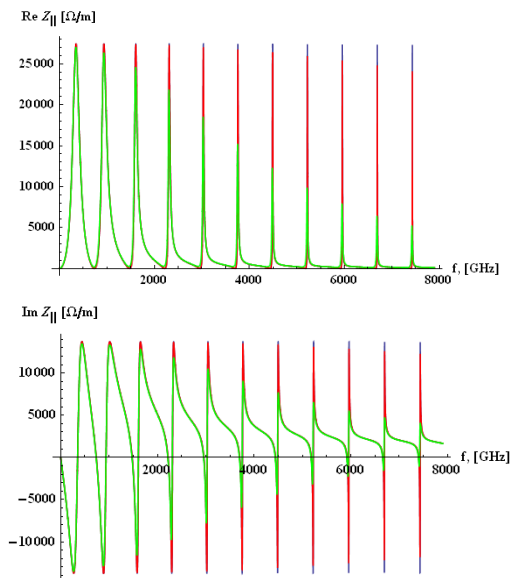


Figure 2: Real (top) and imaginary (bottom) parts of longitudinal impedance of ceramic tube with external metallic layer. Layer conductivities: $\sigma = 58 \cdot 10^9$ (blue), $\sigma = 58 \cdot 10^6$ (red) and $\sigma = 58 \cdot 10^3$ (green) $\Omega^{-1} \cdot \text{m}^{-1}$

The impedance is characterized by the periodically located narrow-band peaks with damped amplitudes. The

damping rate increases with the outer layer conductivity reduction. The periodicity of impedance distribution is conditioned by term $\operatorname{tg}(k d_2 \varepsilon'')$ (6), i.e. depends only on the parameters of dielectric layer (the same is true for the dielectric-metal two-layer tube [5]). The period is equal to $\Delta k = \pi/d_2 \varepsilon''$. At the discrete periodical frequencies $k = \pi/d_2 \varepsilon'' l, l = 1, 2, \dots$ the impedance is independent of the parameters of dielectric layer and is equal to the impedance of waveguide with outer metallic layer with thickness equal to d_3 and inner radius a_3 . At the points $k = \pi/d_2 \varepsilon'' (l + 1/2)$ ($\operatorname{tg}(k d_2 \varepsilon'') \rightarrow \infty$) the impedance reaches its extreme values, the level of which, in contrary, strongly depends on all layers parameters.

The presence of thick inner metallic coating leads to abrupt falling of radiation intensity and to smoothing of impedance curves at low frequencies (Fig.3). In this case the middle ceramic layer impact is limited by skin effect in the inner metallic layer: in low frequency region ($f < f_s$) ($f_s = 1/\pi\mu_0\sigma_1 d_1^2$ is the frequency, at which the layer thickness is equal to a skin depth) the impedance is mostly conditioned by the ceramic and outer metallic layers summary influence, while in the opposite case ($f > f_s$) the inner metallic layer impact is determinative. Thus, the impedance distribution should strongly depend on the inner layer thickness and its filling. Fig. 3 presents the case of high conductivity of inner layer ($\sigma_1 = 58 \cdot 10^6 \Omega^{-1} \cdot \text{m}^{-1}$, copper). In this case the impact of ceramic is almost invisible.

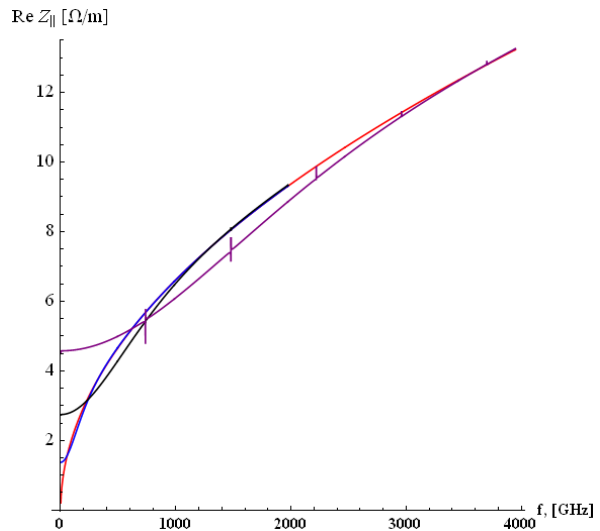


Figure 3: Real part of three-layer tube longitudinal impedance; impedance of copper tube (red); $d_1 = 1 \mu\text{m}, f_s = 4.4 \text{ GHz}$ (blue); $d_1 = 0.5 \mu\text{m}, f_s = 17.5 \text{ GHz}$ (black); $d_1 = 0.3 \mu\text{m}, f_s = 48.5 \text{ GHz}$ (orange).

The increasing of the frequency region with ceramic layer substantial impact may be reached by reduction of the inner layer thickness or its conductivity. The cases of low

conducting inner cover ($58 \cdot 10^3 \Omega^{-1} \text{m}^{-1}$) are presented on Fig. 4 and Fig. 5.

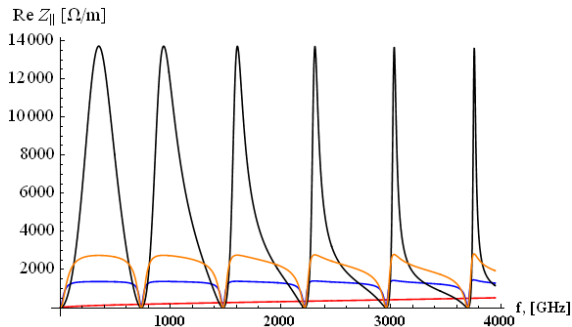


Figure 4: Real part of three-layer tube longitudinal impedance; impedance of low-conducting tube (red); $d_1=1 \mu\text{m}$, $f_s=4.4 \text{ THz}$, (blue), $d_1=0.5 \mu\text{m}$, $f_s=17.5 \text{ THz}$ (orange); $d_1=0, 1 \mu\text{m}$, 437 THz (black).

The above consideration is in case of copper outer layer. The impedance curve deformations with its changing by low conducting layer are shown below.

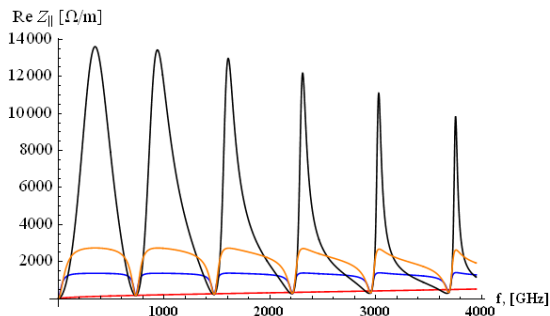


Figure 5: Real part of three-layer tube longitudinal impedance; impedance of low-conducting tube (red); $d_1=1 \mu\text{m}$, $f_s=4.4 \text{ THz}$, (blue), $d_1=0.5 \mu\text{m}$, $f_s=17.5 \text{ THz}$ (orange); $d_1=0, 1 \mu\text{m}$, 437 THz (black).

The main conclusion, which follows from the comparison of Fig. 4 and Fig. 5 is that the influence of outer layer is the most sensitive in thin inner layer case. Thus, to get a quazi-periodical frequency distribution with high amplitudes the outer high conducting and inner low conducting thin layers should be chosen.

WAKE POTENTIALS

Related to the two-beam acceleration, the importance of the longitudinal wake potentials is in possibility of clarification of the allowable arrangement of driving charge (choosing the optimal distance between the driving and driver charges) and determination of the acceleration rate.

The short range longitudinal wake potentials for the discussed three-layer waveguide (for the point-like charge) corresponding to both cases ($\sigma_3=58 \cdot 10^6$ and

$\sigma_3=58 \cdot 10^3 \Omega^{-1} \text{m}^{-1}$) presented in Fig.4 and Fig.5 are plotted on Fig. 6. The conductivity value of outer layer does not act significantly on the short range wake distribution. The case of $d_1=0.1 \mu\text{m}$ should be noted especially. The significant difference of impedance distribution (compare black curves in Fig 4 and Fig.5) do not cause notable changes of wake potentials in the frame of considered distances ($s \leq 600 \mu\text{m}$). Taking into account the theorem of unambiguity of Fourier transform, the difference should be apparent at long distances (long range wake). The on-charge field value stays independent of both the inner and outer layer electro-dynamical and geometrical parameters.

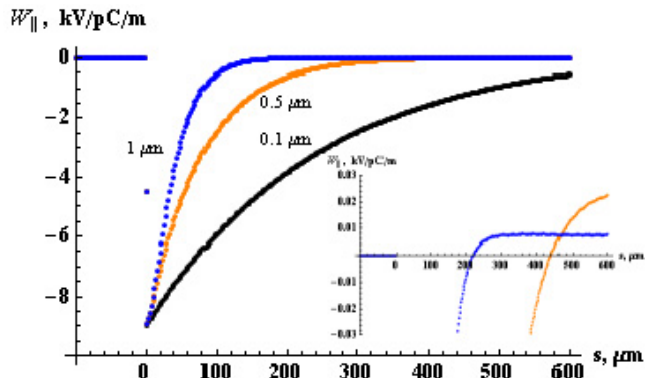


Figure 6: Longitudinal wake potentials for three layer ceramic waveguide. The accelerated (positive) parts of wake potentials for $d_1=1 \mu\text{m}$ (blue) and $d_1=0.5 \mu\text{m}$ (orange) are plotted separately.

As it is seen from the additional plots in Fig. 6, the thicker inner metallic cover corresponds to large accelerating distances with higher voltages.

CONCLUSION

The main regularities of changing of longitudinal impedance and wake potential of metallized three-layer ceramic waveguide with modification of its main geometrical and electro-dynamical parameters are obtained. Now it is possible to choose the optimal parameters of discussed waveguide to obtain the maximal accelerating rate. Of course, additional investigations should be performed to get the agreement with transverse stability and with the acceptable thermal regime as well. In addition, long range wake should be calculated and optimised related to the multibunch acceleration case.

REFERENCES

- [1] Wei Gai et al, EPAC01, p. 1880-1882.
- [2] Wei Gai, eprint arXiv: Physics/0004077 v1, 28 Apr 2004.
- [3] SLAC, private communication.
- [4] M. Ivanyan et al, PRST-AB, 11, 084001 (2008)
- [5] A. Tsakanian, J. Rossbach, M. Ivanyan, EPAC08, p. 1712- 1714.